Cancer Research

Ubiquitous Release of Exosomal Tumor Suppressor miR-6126 from Ovarian Cancer Cells

Pinar Kanlikilicer[1,2], Mohammed H. Rashed[1,3], Recep Bayraktar[1], Rahul Mitra[2,4], Cristina Ivan[1,2], Burcu Aslan[1,2], Xinna Zhang[2,4], Justyna Filant[4], Andreia M. Silva[1], Cristian Rodriguez-Aguayo[1,2], Emine Bayraktar[1], Martin Pichler[1,5], Bulent Ozpolat[1,2], George A. Calin[1,2,6], Anil K. Sood[2,4,6], and Gabriel Lopez-Berestein[1,2,6]

Abstract

Cancer cells actively promote their tumorigenic behavior by reprogramming gene expression. Loading intraluminal vesicles with specific miRNAs and releasing them into the tumor microenvironment as exosomes is one mechanism of reprogramming whose regulation remains to be elucidated. Here, we report that miR-6126 is ubiquitously released in high abundance from both chemosensitive and chemoresistant ovarian cancer cells via exosomes. Overexpression of miR-6126 was confirmed in healthy ovarian tissue compared with ovarian cancer patient samples and correlated with better overall survival in patients with high-grade serous ovarian cancer. miR-6126 acted as a tumor suppressor by directly targeting integrin-β1, a key regulator of cancer cell metastasis. miR-6126 mimic treatment of cancer cells resulted in increased miR-6126 and decreased integrin-β1 mRNA levels in the exosome. Functional analysis showed that treatment of endothelial cells with miR-6126 mimic significantly reduced tube formation as well as invasion and migration capacities of ovarian cancer cells *in vitro*. Administration of miR-6126 mimic in an orthotopic mouse model of ovarian cancer elicited a relative reduction in tumor growth, proliferating cells, and microvessel density. miR-6126 inhibition promoted oncogenic behavior by leading ovarian cancer cells to release more exosomes. Our findings provide new insights into the role of exosomal miRNA-mediated tumor progression and suggest a new therapeutic approach to disrupt oncogenic phenotypes in tumors. *Cancer Res; 76(24); 7194–207. ©2016 AACR.*

Introduction

Exosomes are nano-sized vesicles shed from living cells, initially considered a mechanism for discarding cell debris (1). A significant body of evidence has demonstrated that these vesicles can transfer their contents to and modify the phenotype of host cells (2), thereby acting as intracellular communication devices (3). Increasing evidence supports multiple roles for exosomes, such as promoting or suppressing tumorigenesis. Tumor-derived exosomes can promote tumor immunoevasion through induction of T-cell apoptosis (4). Exosomes isolated from bladder cancer cell lines exhibited dose- and time-dependent inhibition of apoptosis by upregulation of Bcl-2 and cyclin D1 proteins (5). Exosomes can contribute to cancer growth by enhancing anti-apoptotic and other oncogenic pathways such as angiogenesis, invasion, and metastasis (6–8). In contrast, tumor cells have been shown to release exosomes containing tumor antigens that then induce antitumor immune responses (9–13). Hence, the functions of the exosomes most likely depend on the cargo and their regulation.

Noncoding RNAs such as microRNA (miRNA) have been reported to exert tumor suppressor or oncogenic functions (14–17). Circulating miRNAs in serum can be used as diagnostic markers for various cancer types (18–20). Extensive miRNA profiling of circulating exosomes from body fluids of patients with cancer showed that many exosomal proteins or miRNAs are also involved in various cancers such as those of the breast, prostate, and ovary (21–24).

There are 2 potentially nonexclusive hypotheses regarding how exosome-mediated miRNA transfer contributes to cancer. Malignant cells use exosomes as vehicles to release (i) their tumor suppressor miRNAs or (ii) oncogenic miRNAs—to maintain and protect the oncogenic potential of the cancer cells. Our purpose was to elucidate the function of exosomal miRNAs and shed light on their role in tumor/microenvironment homeostasis.

In the current study, using miRNA expression profiling of chemosensitive and chemoresistant ovarian cancer cell lines, we identified miR-6126 as a novel tumor suppressor that cells discard via exosomes. We discovered that ectopic expression of miR-6126 inhibits many oncogenic functions of ovarian cancer cells, such as proliferation, invasion, migration, and angiogenesis. Identification of increased levels of miR-6126 in the exosomes released by

[1]Department of Experimental Therapeutics, The University of Texas MD Anderson Cancer Center, Houston, Texas. [2]Center for RNA Interference and Non-Coding RNA, The University of Texas MD Anderson Cancer Center, Houston, Texas. [3]Department of Pharmacology and Toxicology, Faculty of Pharmacy, Al-Azhar University, Cairo, Egypt. [4]Department of Gynecologic Oncology and Reproductive Medicine, The University of Texas MD Anderson Cancer Center, Houston, Texas. [5]Division of Oncology, Medical University of Graz, Austria. [6]Department of Cancer Biology, The University of Texas MD Anderson Cancer Center, Houston, Texas.

Note: Supplementary data for this article are available at Cancer Research Online (http://cancerres.aacrjournals.org/).

Corresponding Author: Gabriel Lopez-Berestein, Department of Experimental Therapeutics, 1901 East Road, Unit 1950, The University of Texas MD Anderson Cancer Center, Houston, TX 77030. Phone: 713-792-8140; Fax: 713-792-0362; E-mail: glopez@mdanderson.com

doi: 10.1158/0008-5472.CAN-16-0714

ovarian cancer cell lines in our study conforms to the hypothesis that malignant cells release their *tumor suppressor miRNAs* via exosomes into the extracellular environment to maintain and promote tumorigenesis at the intracellular level.

Materials and Methods

Cell lines and patient samples

RPMI medium supplemented with 10% FBS and 100 IU/mL penicillin/streptomycin was used as the culture medium for the HeyA8, SKOV3-ip1, and A2780 ovarian cancer cell lines. Taxane-resistant HeyA8-MDR and SKOV3-TR ovarian cancer cell lines were maintained in RPMI medium supplemented with 10% FBS and 1% penicillin/streptomycin with added paclitaxel (300 ng/mL for HeyA8-MDR and 150 ng/mL for SKOV3-TR). The A2780-CP20 ovarian cancer cell line was developed and maintained as previously described (25). The immortalized human endothelial RF-24 (EC-RF24) cell line was maintained in minimal essential medium (MEM) supplemented with 10% FBS, 1% MEM vitamins, 1% L-glutamine, 1% sodium pyruvate, and 1% nonessential amino acids. All cells were maintained at 37°C with 5% CO_2 and 95% air and screened for mycoplasma using a MycoAlert mycoplasma detection kit (Lonza Rockland) as described by the manufacturer. All experiments were conducted when cells were 70% to 80% confluent. All cell lines were kindly provided by Dr. Anil K. Sood [The University of Texas MD Anderson Cancer Center (MDACC), Houston, TX]. They were all expanded, cryopreserved, and used within 6 months of recovery from cryopreservation. The authentication of all cell lines was done by the Characterized Cell Line Core Facility at MDACC.

Samples of ovarian tumors ($n = 19$) and normal ovarian surface epithelium (n = 6) from human donors were obtained from Saitama Medical University (Saitama, Japan) and MDACC. Each patient's cancer was staged according to the International Federation of Gynecology and Obstetrics surgical staging system. Supplementary Table S1 includes stage, grade, and histology of the tumors. Normal samples are normal ovarian surface epithelium or normal fallopian tube epithelium. Finally, patient data and mRNA and miRNA expression values for 129 late-stage high-grade serous ovarian cancers profiled with Illumina arrays (E-MTAB-386) were obtained from the GEO information system (26).

Extraction of exosomes from cell culture media

All ovarian cancer cell lines (HeyA8, HeyA8-MDR, SKOV3-ip1, SKOV3-TR, A2780, A2780-CP20) were plated in cell culture medium containing 10% FBS and cultured for 24 hours to 70% confluence. The medium from each culture was replaced with 10% exosome-depleted FBS and cells were grown for 24 hours more. The medium from each culture was then subjected to centrifugation at 2,000 × *g* for 30 minutes to remove cell debris. The resulting cell-free medium was combined with a half volume of total exosome isolation reagent (Invitrogen) and mixed well by subjecting to vortexing until a homogenous solution was formed. The samples were incubated at 4°C overnight and then subjected to centrifugation at 10,000 × *g* at 4°C for 1 hour. The supernatants were aspirated, and the exosome pellets were resuspended in PBS buffer and stored at −20°C.

Western blotting

Cell lysates were subjected to centrifugation, and the supernatants were collected and their protein concentration determined by using the BCA protein assay (Pierce). Protein samples were subjected to electrophoresis on polyacrylamide gels (Bio-Rad) and then transferred to polyvinylidene fluoride membranes (Bio-Rad). Membranes were blocked, rinsed, and incubated with primary antibodies against p-PI3K$_{Y458}$, p-AKT$_{S473}$, AKT, VEGFR2, MMP2, p-c-RAF$_{S2590}$, p-c-RA $_{S289/296/301}$, c-RAF, integrin-β1, t-paxillin, and p-paxillin $_{Y118}$ (Cell Signaling Technology). After overnight incubation at 4°C, membranes were washed and incubated with their corresponding secondary antibody conjugated with horseradish peroxidase. Protein bands were detected with an enhanced chemiluminescence detection kit (GE Healthcare). β-Actin was used as the loading control.

miRNA transfection

Ovarian cancer cells were plated at a density of 8×10^4 cells per well in 6-well plates. The next day, cells were transfected with 50 nmol/L control miRNA mimic or miR-6126 mirVana mimic (Life Technologies) for 48 hours using HiPerFect transfection reagent (Qiagen). Invasion, wound healing, tube formation, and EdU assays that were performed following miRNA transfection are explained in Supplementary Methods.

miRNA microarray and gene expression analysis

RNAs from exosomes were isolated by using the miRCURY Exosome Isolation Kit (Exiqon). RNA samples were quantified by using a NanoDrop spectrophotometer (Thermo Scientific), and quality was assessed on a Bioanalyzer (Agilent Genomics). Hybridization and scanning of the samples were performed by the Noncoding RNA Program at the Center for Targeted Therapy, MDACC, using 4.0 miRNA Affymetrix chips. Microarray data were submitted to GEO database (GSE76449). The microarray data were validated by quantitative RT-PCR (qRT-PCR). Processing of the microarray data and qRT-PCR are explained in Supplementary Methods.

Reverse-phase protein array

Reverse-phase protein array (RPPA) was performed by the MD Anderson RPPA Core Facility. Experimental details are described in Supplementary Methods.

Animal studies

Female athymic nude mice were injected intraperitoneally with HeyA8 cells (1×10^6 cells/mouse) and then randomly assigned to 1 of 2 treatment groups: control miRNA mimic or miR-6126 mimic. miRNAs were incorporated into DOPC liposomes, and mice were injected with miRNA (200 μg/kg/mouse) twice weekly starting 1 week after tumor inoculation. Mice were killed when moribund or 5 weeks after initial injection of tumor cells. Histologic staining of their tissues was performed by the MD Anderson Histology Core facility. The animal experiments were conducted in accordance with American Association for Laboratory Animal Science regulations and with the approval of the Institutional Animal Care and Use Committee of MDACC.

Immunohistochemistry

Unstained sections of mouse tissue were deparaffinized and rehydrated. Antigen retrieval was performed using Dako antigen retrieval solution (Dako North America). Endogenous peroxidase was blocked using 3% hydrogen peroxide. Tissues were incubated with primary antibodies against Ki67 (Thermo/Lab Vision Corp.)

and CD31 (Abcam) overnight at 4°C. Next day, a goat anti-rabbit horseradish peroxidase secondary antibody (Jackson ImmunoResearch Laboratories) diluted in blocking solution was added and the samples were incubated for 1 hour at room temperature. Slides were developed with DAB substrate (Vector Laboratories, Inc.) and counterstained with Gill no. 3 hematoxylin solution. Positive (DAB-stained) cells were counted in 5 random fields per slide.

Statistical analysis

Quantitative data are presented as the means ± SD of 3 independent experiments. Quantitative data for different groups were compared by the Student *t* test, and $P < 0.05$ was considered significant. The normality of the distribution was tested by using the Shapiro–Wilk test. The Fisher exact test was used to identify the significance of differences in identified molecular and cellular functions.

Survival analyses were performed in R (version 3.0.1; http:///www.r-project.org/). Patients were grouped into percentiles according to mRNA/miRNA expression. The log-rank test was employed to determine the association between mRNA/miRNA expression and overall survival, and the Kaplan–Meier method was used to generate survival curves. Cutoff points to significantly divide (log-rank test: $P < 0.05$) the samples into low/high mRNA/miRNA groups were determined, and the optimal cutoffs were chosen as the minimum *P* values: 0.3 for *ITGB1* (ILMN_1723467) and 0.61 for miR-6126. We also fixed the *ITGB1* and miR-6126 cutoff levels, which split the cohort into 4 groups corresponding to low/high gene and low/high miRNA expression. We contrasted the 2 groups with a negative association: high *ITGB1*/low miR-6126 expression with low *ITGB1*/high miR-6126 expression. The Spearman rank-order correlation test was applied to measure the strength of the association between *ITGB1* and miR-6126.

Results

miR-6126 is differentially expressed in ovarian cancer exosomes and ovarian cancer cell lines

To identify the oncogenic and tumor suppressor miRNAs differentially expressed in exosomes and their cells of origin, we first isolated miRNAs from exosomes that were characterized by atomic force microscopy and transmission electron microscopy (Supplementary Fig. S1A and S1B). We then performed comprehensive miRNA expression profiling of 3 pairs of chemotherapy-sensitive and -resistant ovarian cancer cell lines (SKOV3-ip1 and Skov3-TR, HeyA8 and HeyA8-MDR, A2780 and A2780-CP20) using the Affymetrix miRNA 4.0 array. After background adjustment and quantile normalization were applied, one-way ANOVA was performed to identify human mature miRNAs that were significantly differentially expressed in the exosomes and their cells of origin. Differences in miRNA expression levels were considered significant at $P < 0.05$ and fold change >2 or ←2.

In all exosomes derived from the sensitive ovarian cancer cells (HeyA8, SKOV3-ip1, A2780), miR-6126 expression levels were significantly higher than those in their cells of origin, whereas miR-92a-1-5p, miR-30c-5p, and let 7d- 5p expression levels were significantly lower in the exosomes than in their cells of origin (Fig. 1A). For exosomes derived from the resistant ovarian cancer cells (HeyA8-MDR, SKOV3-TR, A2780-CP20), 11 mature human miRNAs (miR-122-5p, miR-4459, miR-4484, miR-4487, miR-4530, miR-1246, miR-1268a, miR-6126, miR-6769b, miR-7107-5p, and miR-7150) were significantly upregulated, whereas 3 miRNAs (miR-125a-5p, miR-4485, and miR-30c-5p) were significantly downregulated (Fig. 1A) compared with their cells of origin. We identified one miRNA, miR-6126, as significantly enriched ($P < 0.05$, fold change > 2) in all the exosomes derived from all 6 ovarian cancer cells as compared with their cells of origin (Fig. 1B).

Next, we performed Kyoto Encyclopedia of Genes and Genomes (KEGG) pathway analysis for the mRNA targets of these miRNAs to find enriched pathways. mRNA targets of miRNAs of interest were obtained using TargetScan database (version 7.0, www.targetscan.org). The most enriched pathways were sorted by the *z*-scores (Fig. 1C). For the sensitive ovarian cancer cells, the many significantly enriched cancer-related pathways for mRNAs that were targeted by upregulated miRNAs included microRNAs in cancer, Notch signaling, cell cycle, p53 signaling, and MAPK signaling, whereas for mRNAs targeted by downregulated miRNAs, the significantly enriched pathways were related to PPAR signaling, fatty acid metabolism, and biosynthesis of amino acids. For the resistant ovarian cancer cells, the enriched tumor-related pathways for mRNAs targeted by upregulated miRNAs included PPAR signaling and those for the mRNAs targeted by downregulated miRNAs included TNF signaling and NF-κB signaling.

The expression levels of miR-6126, which was upregulated in all exosomes from 6 different ovarian cancer cell lines (Supplementary Table S2), were validated by qPCR (Fig. 2A). We also compared the expression levels of miR-6126 in ovarian cancer cell line–derived exosomes with those derived from normal ovarian epithelial ovarian cell lines (HIO180) by qPCR and found that the exosomes from A2780-CP20, HeyA8, HeyA8-MDR, and SKOV3-ip1 cell lines expressed more miR-6126 than the exosomes from HIO180 (Fig. 2B). The increased expression of miR-6126 in those exosomes prompted us to investigate the role of miR-6126 in cancer because the miRNA data suggested that miR-6126 may play a major role in ovarian cancer cell survival, invasion, microenvironment, and tumorigenesis.

To further define the potential effect of miR-6126 in patients with ovarian cancer, we analyzed all available data to determine the correlation of miR-6126 with patient survival. In the ArrayExpress data, expression of miR-6126 in the tumor was inversely correlated with tumor progression in patients with ovarian cancer (Fig. 2C). The 50% survival rates of patients with high miR-6126 expression and those with low expression differed by almost 18 months. We also measured miR-6126 expression levels in patient tumor samples ($n = 19$) by qRT-PCR and compared them with levels in normal tissues ($n = 6$). Normal samples are normal ovarian surface epithelium or normal fallopian tube epithelium. miR-6126 expression levels were significantly lower in tumors than in normal tissues (Fig. 2D).

PI3K/AKT signaling is altered by ectopic expression of miR-6126

We performed RPPA to define the proteomic effect of miR-6126 in HeyA8 ovarian cancer cells. Cells were transfected with either control miRNA mimic or miR-6126 mimic for 48 hours, and cell lysates were processed for RPPA analysis. The canonical pathway analysis showed that multiple pathways related to cancer signaling were altered upon miR-6126 transfection in the HeyA8 cells (Fig. 3A). The PI3K/AKT signaling and PTEN signaling pathways were the top 2 most significantly enriched pathways in the dataset. Correspondingly, our immunoblotting results in miR-6126–

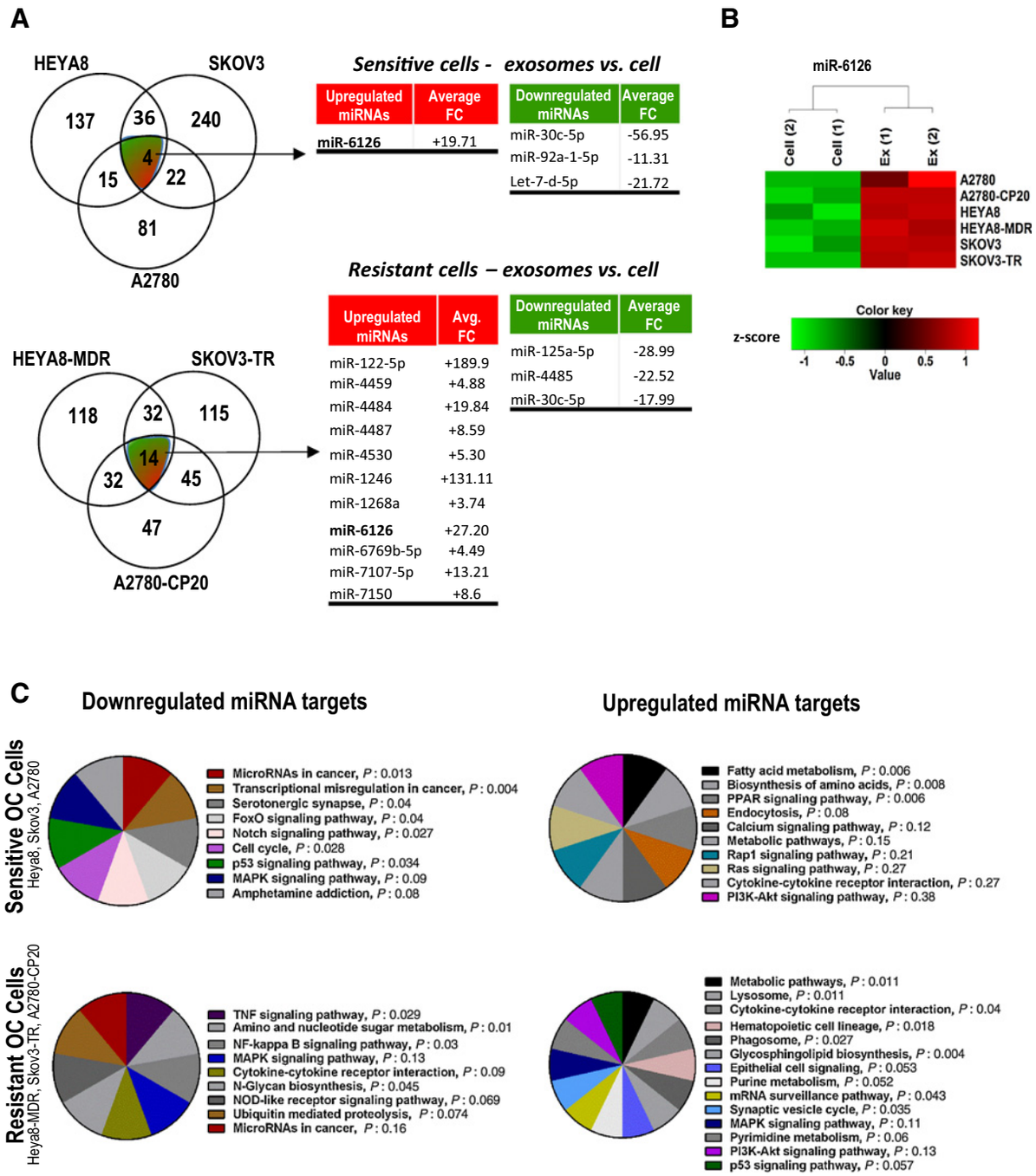

Figure 1.

Analysis of microRNAs in cancer exosomes and their cells of origin. **A,** Common miRNAs were significantly differentially expressed between exosomes and their cell of origin for chemosensitive parental ovarian cancer cells (top) and chemoresistant ovarian cancer cells (bottom). FC, fold change. **B,** *z*-scores of miR-6126 (Supplementary Table S3) in six different cancer exosomes and their cells of origin. The rows represent individual ovarian cancer cell lines, and the columns represent the cellular compartments of miR-6126 expression. Negative *z*-scores are shown in green, positive *z*-scores in red. **C,** KEGG pathway analysis of the target mRNAs of significantly differentially regulated miRNAs is common for both sensitive ovarian cancer cells (top; HeyA8, SKOV3-ip1, A2780) and resistant ovarian cancer cells (bottom; HeyA8-MDR, SKOV3-TR, A2780-CP20). OC, ovarian cancer.

transfected HeyA8 cells showed decreases in p-PI3K (Y458), whereas PTEN levels did not change (data not shown). Transfection with miR-6126 mimic reduced the levels of phosphorylated PI3K and AKT in the resistant HeyA8-MDR cells and in SKOV3-ip1 and SKOV3-TR cells (Fig. 3C). Further analysis of the PI3K/AKT signaling pathway in RPPA data showed reductions in c-RAF

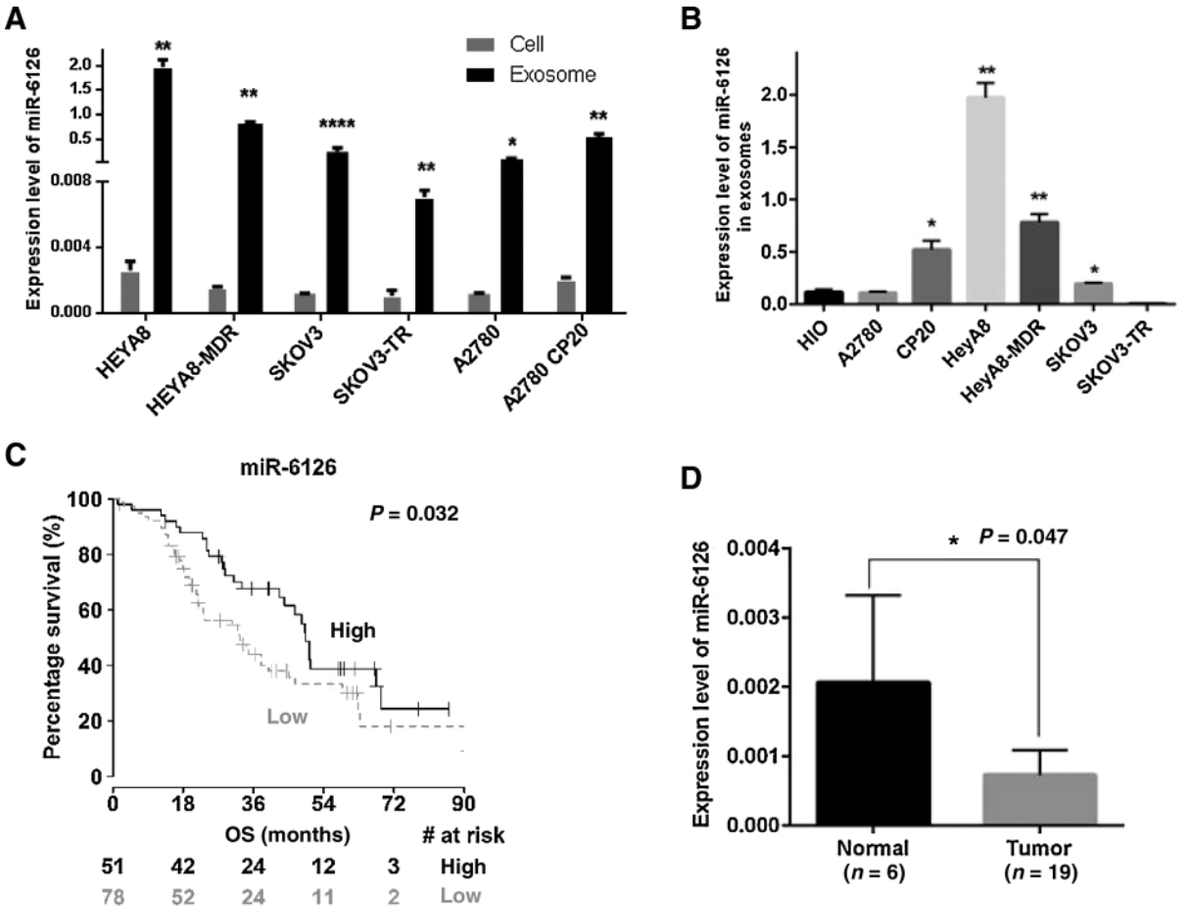

Figure 2.

miR-6126 expression in exosomes from cancer cells and in patient tissue. **A,** qPCR validation of miR-6126 expression in exosomes and cells of origin for all cancer cell lines used in the microarray experiment. **B,** Comparison of miR-6126 expression in exosomes derived from ovarian cancer cells and in exosomes derived from immortalized normal human ovarian surface epithelial cells (HIO180) by qPCR. **C,** Low expression of miR-6126 was associated with shorter survival in patients with ovarian cancer, as shown by Kaplan–Meier analysis of miR-6126 expression data extracted from the ArrayExpress database ($P < 0.05$). Cutoff points to significantly split (log-rank test: $P < 0.05$) the samples into low/high mRNA/miRNA groups were recorded. The minimum P values were chosen as cutoffs to optimally separate the patients in high/low groups. The cutoff for ITGB1 (ILMN_1723467) was 0.3 and for miR-6126 was 0.61. **D,** miR-6126 expression in normal ovarian tissues ($n = 6$) and ovarian tumors ($n = 19$) from patients. *, $P < 0.05$; **, $P < 0.01$; ***, $P < 0.001$; ****, $P < 0.0001$.

protein levels in HeyA8 (Fig. 3B), suggesting the role of miR-6126 in cell growth. Our Western blotting results showed that levels of p-c-RAF (S259,S289/296/301) were dramatically decreased by ectopic expression of miR-6126 in drug-resistant ovarian cancer cells (HeyA8-MDR and SKOV3-TR) upon miR-6126 ectopic expression (Fig. 3C) but were altered only slightly or not at drug-sensitive HeyA8 and SKOV3-ip1 cells, respectively. These data suggest that chemoresistant cell lines are more sensitive to miR-6126 treatment than chemosensitive cells.

Ectopic expression of miR-6126 impairs ovarian cancer cell metastasis and proliferation *in vitro*

The presence of PI3K/AKT signaling and VEGF signaling within the significantly enriched canonical signaling pathways guided us to look at the effect of miR-6126 on cell motility, invasion, and angiogenesis. Ovarian cancer cells were transfected with miR-6126 mimic (50 nmol/L) to induce miR-6126 overexpression in ovarian cancer cells, control miRNA mimic was used as a control (Supplementary Fig. S2). First, the potential role of miR-6126 in cancer metastasis was explored via wound-healing and invasion assays. In the wound-healing assay, which measured the involvement of miR-6126 in mediating ovarian cancer cell motility, cells transfected with miR-6126 mimic migrated a significantly shorter distance than cells transfected with control miRNA mimic (Fig. 4A). To determine the effect of miR-6126 on HeyA8 and HeyA8-MDR cell invasiveness, we used the Transwell Matrigel invasion assay system. Percentages of invading cells were 62.4% lower for HeyA8 cells and 56.7% lower for HeyA8-MDR cells than for control cells (Fig. 4B). The effect of miR-6126 on DNA replication was tested by EdU cell proliferation assay. HeyA8 cells transfected with miR-6126 mimic or control mimic for 72 hours were incubated with EdU for 2 hours and their EdU incorporation determined by flow cytometry. EdU incorporation was significantly lower in

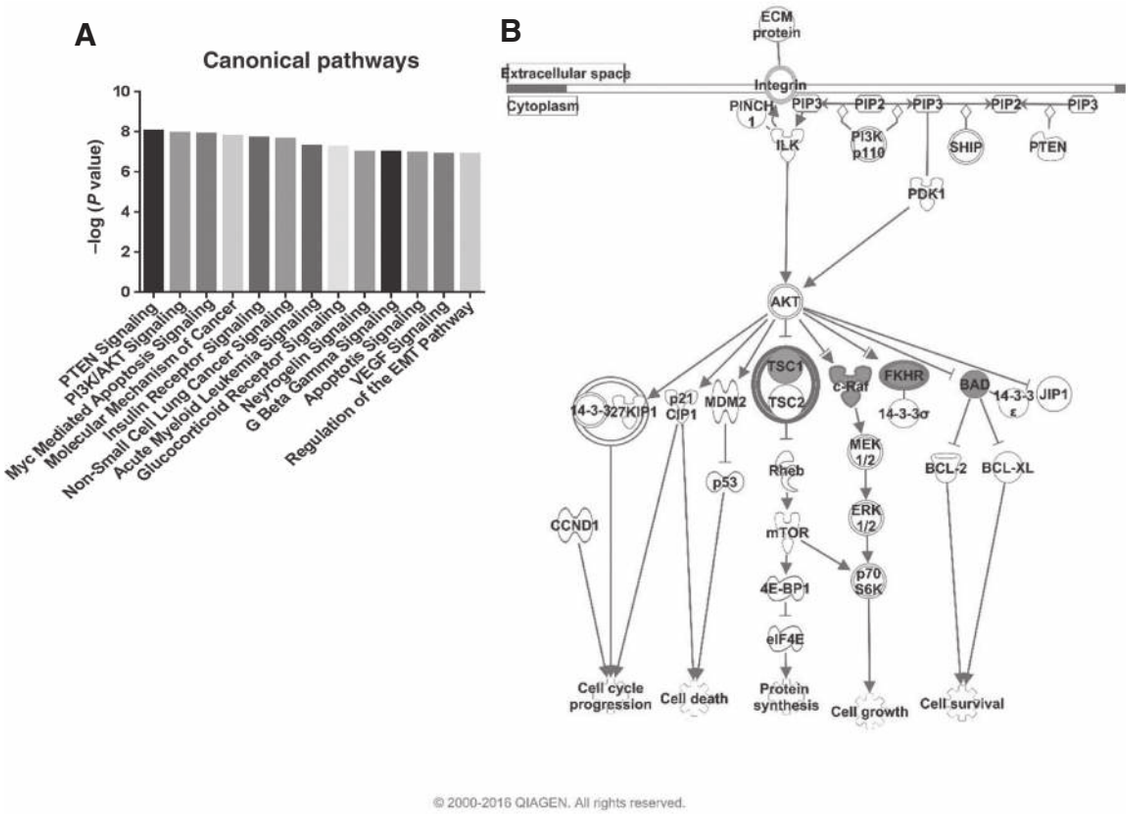

Figure 3.

Proteomic effect of miR-6126 in ovarian cancer cells. **A,** Ingenuity Pathway Analysis of the canonical pathways most enriched in the proteins significantly altered by ectopic expression of miR-6126 in HeyA8 cells; the *y*-axis indicates the $-\log_{10}$ (*P* value) of each enriched pathway. The Fisher exact test was used to calculate *P* value. **B,** PI3K/AKT signaling pathway. Gray, proteins downregulated by miR-6126 transfection in ovarian cancer cells. **C,** Immunoblotting for PI3K/AKT signaling proteins in HeyA8, HeyA8-MDR, SKOV3-ip1, and SKOV3-TR ovarian cancer cells transfected with control miRNA or miR-6126 or no transfection (NT).

miR-6126–transfected cells than in the control miRNA group, indicating that miR-6126 has an antiproliferative effect (Fig. 4C).

We next examined the effect of miR-6126 on angiogenesis, a hallmark of invasive tumor growth and metastasis, by performing an *in vitro* tube formation assay. After incubation on Matrigel for

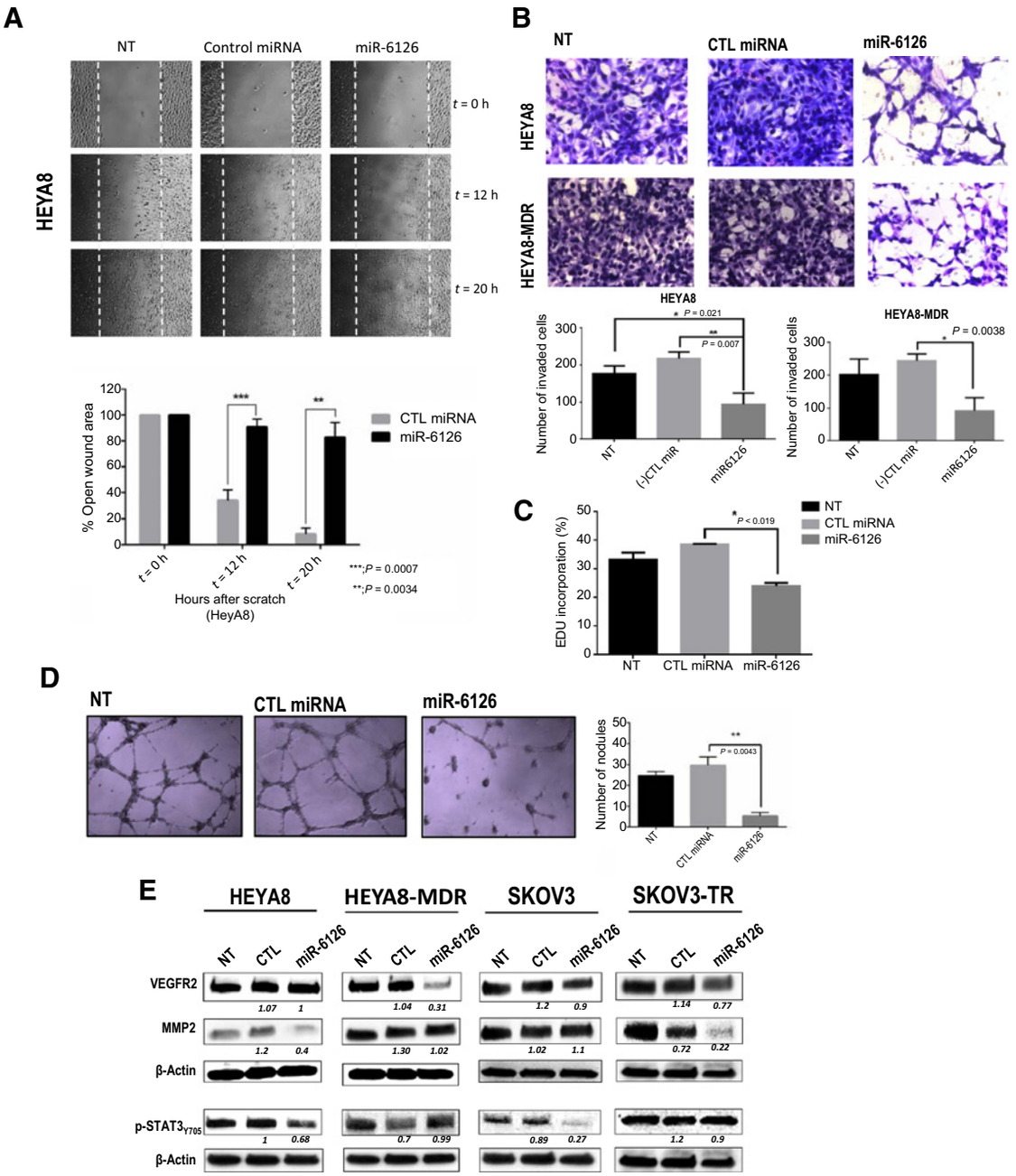

Figure 4.

miR-6126 suppressed migration, invasion, and tube formation of HeyA8 and HeyA8-MDR ovarian cancer cells *in vitro*. **A,** Representative images of *in vitro* wound-healing assay of HeyA8 ovarian cancer cells. Cells were seeded onto 6-well plates and either not transfected (NT) or transfected with control miRNA mimic or miR-6126 mimic. Wound repair was monitored for 24 hours and visualized under microscopy. Images were taken immediately after the scratch was made ($t = 0$ hours) and after 12 and 20 hours. All images shown are representative of three independent experiments; data are presented as mean ± SD of at least three experimental groups. **B,** HeyA8 cells and HeyA8-MDR cells were transfected with control miRNA mimic or miR-6126 mimic. Cells were incubated for 24 hours and invasion was assessed by the Transwell assay. All images shown are representative of three independent experiments; data are presented as mean ± SD of at least three experimental groups. **C,** *In vitro* EdU proliferation assay results for HeyA8 cells transfected with control miRNA mimic or miR-6126 mimic. The transfected cells were incubated 72 hours later with EdU-containing medium for 2 hours, and EdU incorporation was measured by flow cytometry. Data are presented as mean ± SD of at least three experimental groups. **D,** miR-6126 suppressed tube formation in EC-RF24 cells *in vitro*. Transfected EC-RF24 cells were transferred to 8-well culture slides coated with Matrigel (200 μL/well). After 24 hours, the nodes in each culture were counted. All images shown are representative of three independent experiments; data are presented as mean ± SD of at least three experimental groups. **E,** Western blot analysis showing levels of angiogenesis-related proteins in HeyA8, HeyA8-MDR, SKOV3-ip1, and SKOV3-TR ovarian cancer cells transfected with control miRNA mimic or miR-6126 mimic. p-STAT3 was probed on the same membrane used in Fig. 3C for p-PI3K for each corresponding cell line (HeyA8, HeyA8-MDR, and SKOV3-ip1). The same β-actin was used in the top and bottom panels of SKOV3-TR. *, $P < 0.05$; **, $P < 0.01$; ***, $P < 0.001$.

24 hours, immortalized human endothelial EC-RF24 cells transfected with 50 nmol/L miR-6126 mimic exhibited significantly fewer nodes than untreated cells or cells transfected with control miRNA (Fig. 4D), indicating that miR-6126 inhibits *in vitro* angiogenesis. We also analyzed the effects of miR-6126 on levels of angiogenic proteins (VEGFR2, MMP2, p-STAT3) in ovarian cancer cells (Fig. 4E). Levels of VEGFR2 were lower in the miR-6126–transfected groups than in the control miRNA–transfected groups of HeyA8-MDR, SKOV3-ip1, and SKOV3-TR cells. Likewise, p-STAT3 levels were lower in the miR-6126–transfected HeyA8, SKOV3-ip1, and SKOV3-TR cells, whereas MMP2 levels were lower in the miR-6126–transfected HeyA8 and SKOV3-TR cells. Overall, these data indicate that miR-6126 regulates cell migration, invasion, and angiogenesis, which constitute the major steps of metastasis, as well as cell proliferation.

Integrin-β1 a direct target of miR-6126

To determine the mechanism of action for the tumor-suppressing activity of miR-6126, we further examined the proteins involved in PI3K/AKT signaling by computational prediction algorithms and BLAST alignment on their 3′-untranslated regions (UTR). This analysis identified integrin-β1 as a direct target of miR-6126. An 8-base pairing between the *ITGB1* transcript and the miR-6126 sequence was found (Fig. 5A). To confirm this targeting, we first performed immunoblotting for the integrin-β1 protein in HeyA8, HeyA8-MDR, SKOV3-ip1, and SKOV3-TR cells following transfection with miR-6126 mimic (Fig. 5B, Supplementary Fig. S3A). Expression of the integrin-β1 protein was lower in the miR-6126–transfected cells than in the control mimic–transfected cells in all 4 cell types. To determine whether miR-6126 alters integrin-β1 downstream effectors, we examined the effect of miR-6126 transfection on paxillin phosphorylation, which is critical in migration and invasion. miR-6126 transfection inhibited p-paxillin at the tyrosine 118 site in HeyA8-MDR (Fig. 5B), SKOV3-ip1, and SKOV3-TR cells (Supplementary Fig. S3A), whereas there was no difference in HeyA8 cells.

We analyzed the alterations of *ITGB1* induced by miR-6126 overexpression at the transcriptional level and found that miRNA mimic transfection reduced *ITGB1* transcript levels significantly in HeyA8 and HeyA8-MDR cells (Fig. 5C) and in SKOV3-TR cells (Supplementary Fig. S3B). To further confirm that miR-6126 targets *ITGB1*, we used a luciferase reporter assay in which HEK cells were cotransfected with the miR-6126 mimic and with a construct containing *ITGB1*, either wild-type or with multiple mutated nucleotides on the miR-6126–binding sites. Cells transfected with the mutant *ITGB1* construct had no significant reduction in luciferase activity, whereas cells transfected with the wild-type *ITGB1* construct had 18.7% less luciferase activity (Fig. 5D). These results together indicate that miR-6126 targets integrin-β1 in ovarian cancer cells.

Low integrin-β1 and high miR-6126 co-expression result in longer survival

We examined the probability of survival in patients with known *ITGB1* and miR-6126 expression levels (ArrayExpress, E-MTAB-386). Patients were grouped into percentiles according to mRNA/miRNA expression. The log-rank test was used to determine the association between mRNA/miRNA expression and overall survival, and the Kaplan–Meier method was used to generate survival curves. Among 129 patients with late-stage high-grade serous ovarian cancer, 90 had a high tumoral level of *ITGB1* expression and 39 had a low level of *ITGB1* expression (Fig. 5E). A high *ITGB1* level was associated with shorter patient survival. As miR-6126 targets *ITGB1*, we examined the correlation between *ITGB1* and miR-6126 expression and found a significant negative correlation ($r = -0.24$, $P < 0.05$; Fig. 5F). We then split the cohort into 4 groups by setting *ITGB1* and miR-6126 cutoff levels corresponding to low/high mRNA and low/high miRNA expression: low/low, low/high, high/low, and high/high. We then contrasted the 2 groups with a negative association: low/high and high/low. Survival analysis for the combined *ITGB1*/miR6126 expression showed that the difference in survival between these 2 groups was significantly greater than the difference between the groups considered solely on the expression of *ITGB1* or miR-6126 alone (Fig. 5G). When we compared the patients with low *ITGB1* and high miR-6126 expression with patients with high *ITGB1* and low miR-6126 expression, there was a 2-year difference between their 50% survival rates.

Reduced expression of miR-6126 leads to more exosome release

Because there is a correlation between the amount of exosome released and oncogenesis, we examined the effect of miR-6126 inhibition on exosome release by ovarian cancer cells. SKOV3-ip1 cells were transfected with a control miRNA inhibitor or a miR-6126 inhibitor at a final concentration of 100 nmol/L. The medium in each culture was replaced 24 hours after transfection with exosome-depleted medium. Cell supernatants were collected after 48 hours and exosomes were isolated using exosome isolation reagent (Invitrogen). Exosomes were quantified by Nanosight. Our results show that SKOV3-ip1 cells released more exosomes upon miR-6126 inhibition; exosome counts were highest (7.05e+008/mL) for miR-6126 inhibitor–treated cells (Fig. 6A). Cells treated with control miRNA inhibitor released 4.8e+008 exosomes/mL. There were significant differences between cells treated with miR-6126 inhibitor and those not treated or treated with control miRNA inhibitor. However, we observed no significant difference between cells treated with miR-6126 mimic or control miRNA mimic ($P > 0.05$). All samples had a modal ± SD particle diameter of approximately 100 to 120 nm (Fig. 6B). In addition, exosome concentration (particles/mL) by size (nm) was found to be similar for all groups (Supplementary Fig. S4).

Next, we analyzed miR-6126 levels in those vesicles released from SKOV3-ip1 ovarian cancer cells. When we transfected the cells with miR-6126 mimic, exosomes release almost 70-fold more miR-6126 compared with control miRNA mimic–transfected group (Fig. 6C). In addition, those exosomes express significantly lower levels of ITGB1 mRNA, attributable to the inhibition of ITGB1 by mimic miR-6126 (Fig. 6D). When we use miR-6126 inhibitor, we did not observe any significant change in miR-6126 levels in exosomes (Fig. 6C). Moreover, we also compared the basal levels of ITGB1 in exosomes released from SKOV3-ip1 ovarian cancer cells and HIO180 ovarian surface epithelial noncancerous cells, we found significantly higher levels of ITGB1 in cancer exosomes (Fig. 6D). HeyA8, SKOV3-TR, A2780, and A2780-CP20 ovarian cancer cells also express significantly higher ITGB1 levels in their exosomes than in HIO180 exosomes (Supplementary Fig. S5). Altogether, these results suggest that elimination of miR-6126 via cancer exosomes can be a mechanism to block ITGB1 inhibition by miR-6126 in cells.

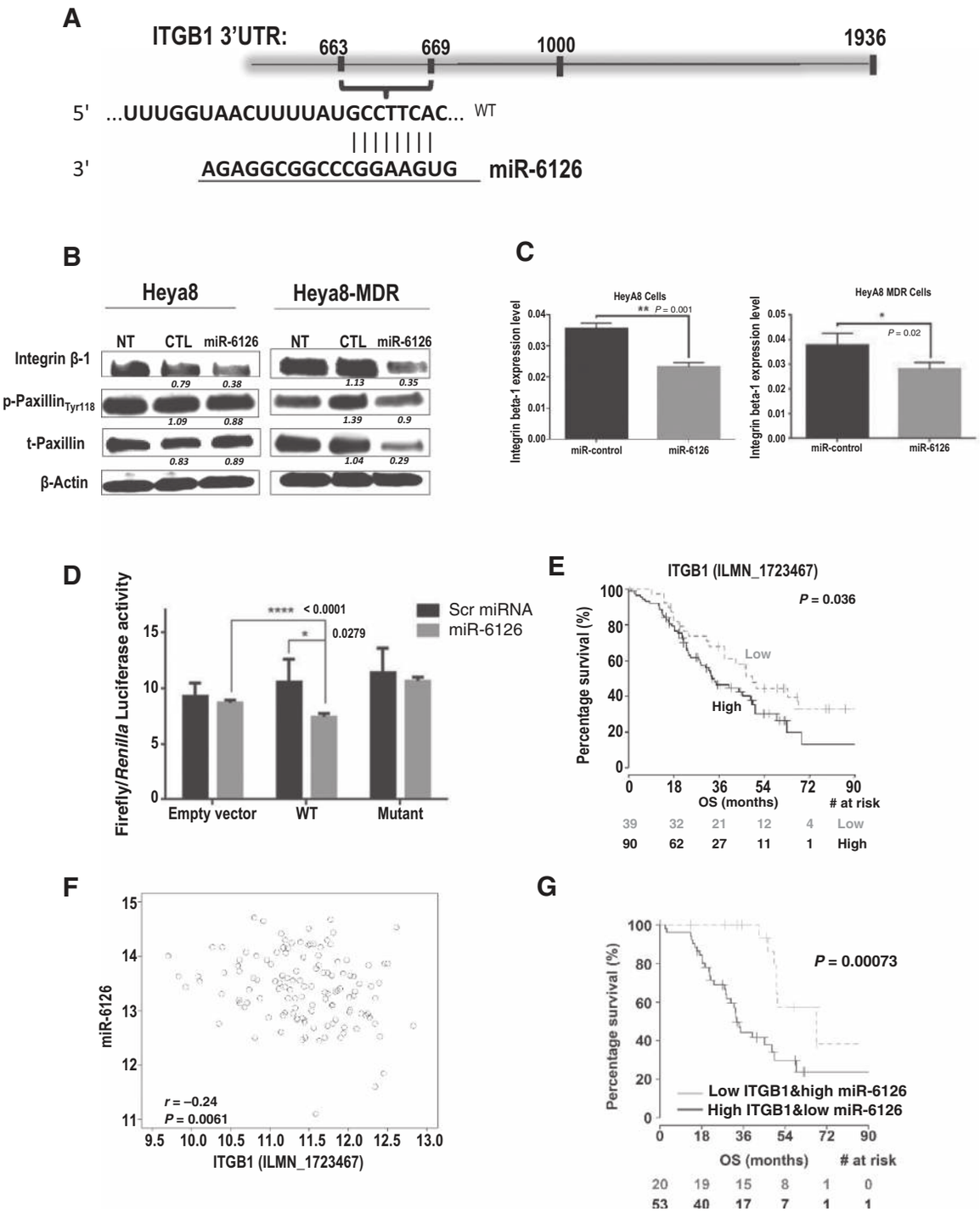

Figure 5.

Integrin-β1 is a direct target of miR-6126. **A,** Predicted binding site for miR-6126 in the 3′-UTR of the integrin-β1 gene *ITGB1*. **B,** Western blot analysis showed the effects of miR-6126 transfection on levels of integrin β-1 protein in HeyA8 and HeyA8-MDR cells. NT, not transfected. Proteins were probed on the same membrane used in Fig. 4E for VEGFR2 and MMP2 proteins for each corresponding cell line (HeyA8 and HeyA8-MDR). **C,** Expression levels of *ITGB1* were determined by qPCR in HeyA8 and HeyA8-MDR cells transfected with miR-6126 mimic. **D,** Firefly luciferase activity in HEK cells cotransfected with a wild-type (WT) or mutant *ITGB1* transcript and with control miRNA mimic or miR-6126 mimic. Data were normalized to *Renilla* luciferase activity. Data are presented as mean ± SD of two biological replicates and three technical replicates. **E,** Association of overall survival (OS) in patients with ovarian cancer with *ITGB1* expression. **F,** miR-6126 expression was negatively correlated with *ITGB1* expression. **G,** Combination of ITGB1/miR6126 gave a better separation than *ITGB1* alone or miR-6126 alone for predicting overall survival. *, $P < 0.05$; **, $P < 0.01$; ****, $P < 0.0001$.

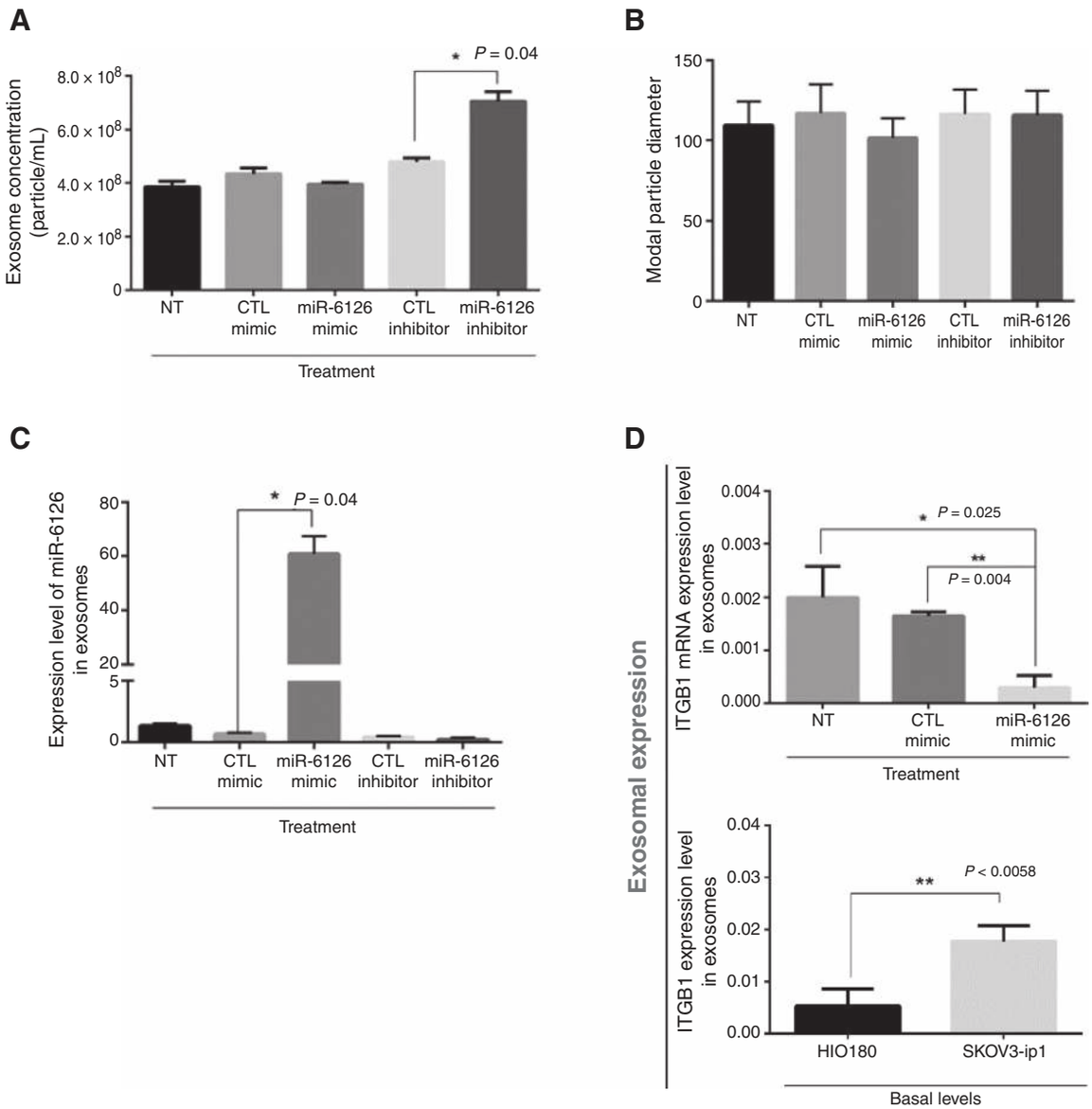

Figure 6.

Exosome release is regulated by miR-6126 in SKOV3-ip1 ovarian cancer cells. **A,** Treatment with miR-6126 inhibitor led to increased exosome release in SKOV3-ip1 ovarian cancer cells. SKOV3-ip1 cells were transfected with miRNA mimics [control (CTL) or miR-6126] or miRNA inhibitors at a final concentration of 100 nmol/L. After 24 hours, the medium was replaced by exosome-depleted medium. After another 48 hours, supernatants were collected and exosomes were isolated using exosome isolation reagent. Particles per milliliter were quantified by Nanosight. Data are presented as mean ± SD of at least two experimental groups. NT, not transfected. **B,** Modal ± SD particle diameter (left) did not differ significantly for exosomes released from cells transfected with control inhibitor/mimic or miR-6126 inhibitor/mimic or negative controls ($P > 0.05$). **C,** miR-6126 expression level in exosomes that were isolated from CTL miRNA- or miR-6126–transfected or not transfected SKOV3-ip1 cells. **D,** ITGB1 mRNA expression levels in exosomes that were isolated from CTL miRNA- or miR-6126–transfected or not transfected SKOV3-ip1 cells. ITGB1 mRNA levels were compared in exosomes isolated from HIO180 (normal) or SKOV3-ip1 ovarian cancer cells. *, $P < 0.05$; **, $P < 0.01$.

miR-6126 inhibits cancer cell proliferation and tumor growth *in vivo*

We assessed the therapeutic efficacy of miR-6126 in an intraperitoneal orthotopic HeyA8 model of ovarian cancer in female athymic nude mice. For *in vivo* systemic administration, miR-6126 mimic and control miRNA mimic were incorporated into DOPC nanoliposomes. Liposomes were injected via tail vein twice a week for 5 weeks. Tumor weights in the miR-6126 mimic–treated group were significantly smaller than those in the control miRNA mimic–treated group (Fig. 7A). No overt toxicity was observed for any treatment group, as indicated by stability of mouse body weight during the therapy (Fig. 7B). We found significantly lower

integrin-β1 levels in tumors treated with miR-6126 mimic than control miRNA mimic–treated group ($P < 0.02$, $P < 0.0016$; Supplementary Fig. S6). We quantified markers of cell proliferation (Ki67) and angiogenesis (CD31) in tumors by immunohistochemistry. miR-6126 treatment led to significant decreases in the numbers of Ki67-positive cells and CD31-positive cells (Fig. 7C). These data support our *in vitro* findings indicating that miR-6126 inhibits proliferation and angiogenesis in ovarian cancer *in vitro* and *in vivo*.

Discussion

Our results demonstrate that miR-6126 was the only miRNA consistently overexpressed in all cancer exosomes released from the 3 different paired ovarian cancer cell lines studied and further show that miR-6126 functions as a regulator of integrin-β1. Higher levels of miR-6126 were associated with longer survival and prognosis in patients with ovarian cancer, suggesting that miR-6126 works as a tumor suppressor in this disease. Our results also show that ectopic expression of miR-6126 resulted in antitumor activity and decreased cell proliferation in ovarian cancer cells *in vivo* and *in vitro*.

The composition of exosomes can be distinct from that of their cells of origin in terms of mRNA, miRNA, and protein contents (27, 28). We found many miRNAs whose expression was significantly higher or lower in ovarian cancer–derived exosomes than in their cells of origin. In an exosomal proteomics study, Hushino and colleagues showed that tumor exosomes are selectively

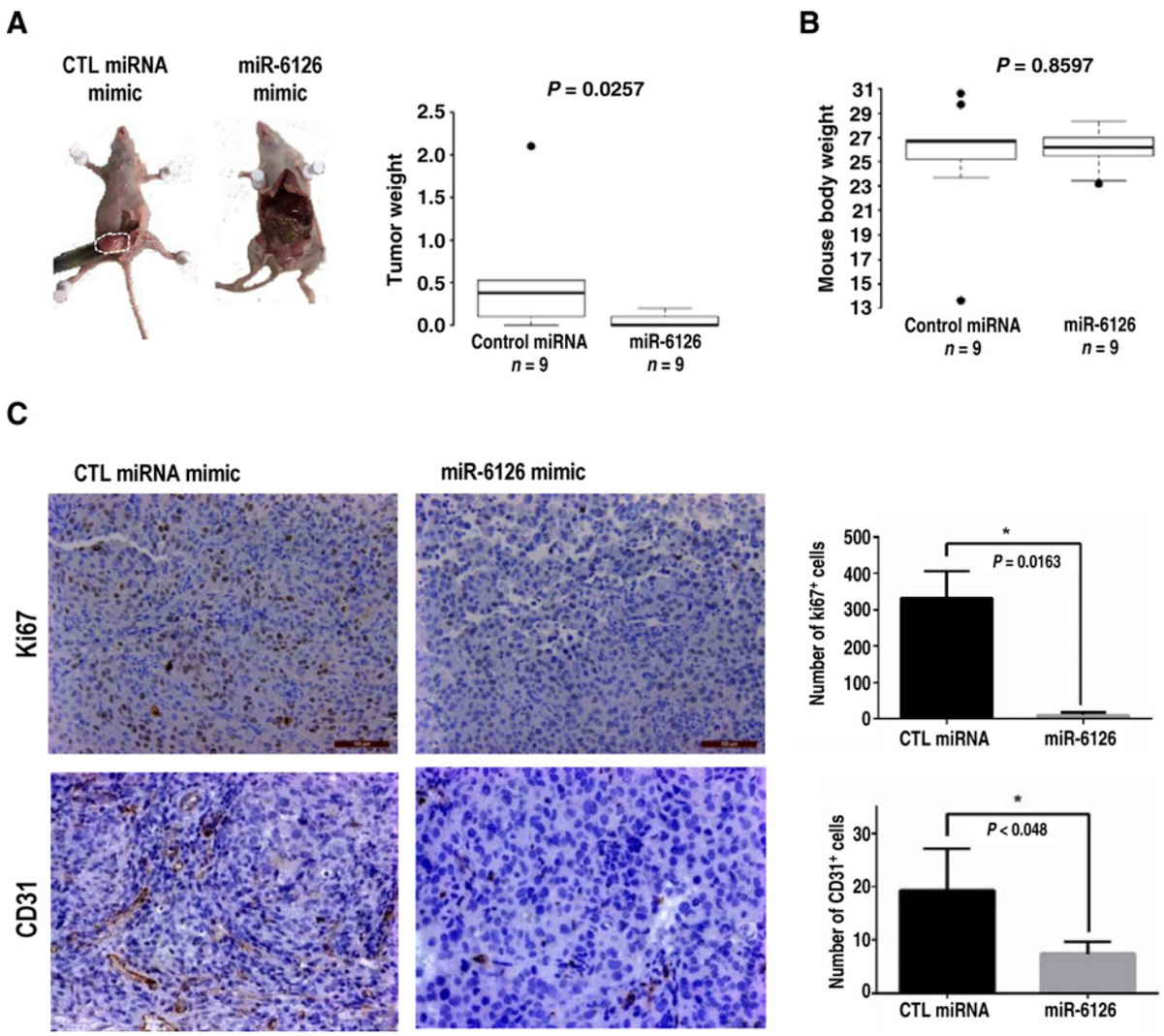

Figure 7.

miR-6126 mimic treatment reduced tumor growth and vasculature in HeyA8 mouse model. **A,** Left, sizes of tumors obtained from representative mice treated with liposomes containing control miRNA mimic or miR-6126 mimic are shown. Right, tumor weights for groups treated with control miRNA mimic or miR-6126 mimic were significantly different ($P < 0.05$, Mann–Whitney–Wilcoxon test). The normality of the distribution was tested by the Shapiro–Wilk test. **B,** Mouse body weights for the groups treated with control miRNA or miR-6126 at the end of the treatment period ($P = 0.857$). **C,** Immunohistochemical staining of markers of proliferating cells (Ki67) and tumor vessel endothelial cells (CD31) in tumors from mice treated with control miRNA mimic or miR-6126 mimic. *, $P < 0.05$.

loaded by a distinct set of integrins to mediate organ-specific tropism (29). Although how these molecules sort into exosomes has not been fully elucidated, Villarroya-Beltri and colleagues recently proposed sequence motifs present in miRNAs that control their localization into exosomes (30). Heterogeneous nuclear ribonucleoprotein A2B1 binds to these motifs via SUMOylation and mediates the sorting of miRNAs into exosomes. However, the mechanism that explains oncogenic versus suppressor-type molecular sorting into exosomes remains to be elucidated.

The machinery for miRNA excretion via exosomes, most likely the identification of short sequence motifs by certain proteins, is abundant in the cytoplasm as shown for cytoplasmic ribonucleoproteins (30), whereas miRNA regulation by transcription may require many proteins and transcription factors. In addition, many studies suggest other complex factors such as regulatory feedback loops that transcriptionally regulates miRNAs (31, 32). Because of the genetic instability in cancer cells, feedback mechanism may be impaired. Therefore, cancer cells may excrete tumor suppressor miRNAs through exosomes. While exosomes as excretion mechanism may be more efficient way for cells to discard unwanted genetic material, transcriptional regulation of miRNAs requires integrated machinery of proteins and other factors. Thus, this might be the reason why cells secrete unwanted miRNAs via exosomes rather than shutting off their transcription.

Exosome-mediated signaling in cancer has been widely studied to elucidate the involvement of exosomes in cancer progression (33–35). As miRNA-mediated posttranscriptional regulation is capable of inducing or inhibiting cancer cell proliferation, metastasis, and progression, the identification of miRNAs in exosomes is important for our understanding of the signaling mechanism of the host cell. Let-7 levels have been shown to be higher in metastatic gastric cancer cell exosomes than in their nonmetastatic counterparts, suggesting that cancer cells promote their oncogenic characteristics by discarding the Let-7 family (15). Another tumor suppressor miRNA, miR-23b, has also been shown to be removed from cancer cells by exosomal pathways to sustain metastatic cascades (16). In another study, oncogenic miR-21 expression was found to be upregulated in exosomes isolated from the serum of patients with esophageal squamous cell cancer, which suggests that miR-21 may serve as a cancer biomarker (36). Our current results highlight the fact that ovarian cancer cells discard specific tumor suppressor miRNAs (as seen by the higher levels of miR-6126 in the exosomes released by ovarian cancer cell lines in our study) and thereby promote their metastatic behavior, confirming the hypothesis that malignant cells release their *tumor suppressor miRNAs* via exosomes into the extracellular environment to maintain and promote tumorigenesis at the intracellular level.

We showed that miR-6126 regulates integrin-β1 as a direct target in ovarian cancer cells. Integrin-β1 receptors are associated with increased invasiveness in many cancers (37–39) and induce cell proliferation and survival (40). PI3K/Akt signaling, the most frequently altered pathway in many cancers (41, 42), was inhibited by miR-6126 and was associated with integrin-β1 protein inhibition. Activation of PI3K/Akt signals has been known to play major roles in migration (43), invasion (44), angiogenesis (45), and proliferation (46). Altered PI3K/AKT signaling and decreased levels of matrix metalloproteinases and VEGF receptor associated with miR-6126 indicate that miR-6126 may prevent extracellular matrix degradation and suppress invasiveness. Correspondingly, *in vitro* functional assays showed that ectopic expression of miR-6126 reduced invasion, migration, and tube formation.

Integrins are proposed as the initiators of the premetastatic niche by directing organ-specific colonization at the host cells of the distant organs (29). This is why it is not surprising that we found higher levels of integrin-β1 mRNA in exosomes released from ovarian cancer cell than in the normal ovarian exosomes. In addition, ectopic expression of miR-6126 in cancer cells leads them to release significantly higher miR-6126 in exosomes, which in turn results in lower integrin-β1 mRNA levels in exosomes. Taken together, these findings suggest a mechanistic approach in which the elimination of miRNA-6126 via exosomes not only promotes oncogenic behavior of the cancer cell but also leads to concurrent downregulation of integrin-β1 mRNA, providing cancer cells to be loaded with more integrin-β1 mRNAs into exosomes, which ultimately mediates metastasis.

Previous studies showed that miRNA-mediated signaling could regulate cancer progression and drug resistance (47). Treatment of drug-resistant non–small cell lung cancer cells with miR-197 mimic sensitized them to chemotherapy. In our study, the effects of miR-6126 on expression levels of proteins involved in cell growth signaling, such as p-c-RAF or p-AKT, were stronger in paclitaxel-resistant (SKOV3-TR) and multidrug-resistant (HeyA8-MDR) cancer cell–derived exosomes than in their sensitive counterparts, indicating the potential role of miR-6126 in chemosensitivity. This observation also may indicate that resistant cell lines are more susceptible to miR-6126–mediated genetic reprogramming.

Cancer cells release more exosomes into the microenvironment than healthier cells (48). Riches and colleagues showed that breast cancer cells released about 50% more exosomes than a human mammary epithelial cell line (49). In a previous study, the number of exosomes isolated from ovarian cancer patient sera was 5-fold higher than that from patients with benign disease (50). Together with our finding that inhibition of tumor suppressor miR-6126 led to an increased release of exosomes in ovarian cancer, these results suggest that the increase in exosome production is associated with an oncogenic response of the cancer cells. Moreover, high expression of miR-6126 in exosomes suggests that cancer cells prevent contribution of specific miRNAs to exosome regulation through sorting these miRNAs into the exosomes in excess amounts.

Our study provides evidence that different types of ovarian cancer cells bearing different type of mutations and displaying different resistance mechanisms release the same tumor-suppressing miR-6126 to the microenvironment in exosomes. These findings show that the exosome-mediated release of tumor suppressor miR-6126 is a potential therapeutic target in ovarian cancer treatment.

Disclosure of Potential Conflicts of Interest

No potential conflicts of interest were disclosed.

Authors' Contributions

Conception and design: P. Kanlikilicer, R. Mitra, A.K. Sood, G. Lopez-Berestein

Development of methodology: P. Kanlikilicer, R. Bayraktar, X. Zhang, J. Filant, C. Rodriguez-Aguayo, G.A. Calin, A.K. Sood, G. Lopez-Berestein

Acquisition of data (provided animals, acquired and managed patients, provided facilities, etc.): P. Kanlikilicer, X. Zhang, J. Filant, C. Rodriguez-Aguayo, E. Bayraktar, M. Pichler, A.K. Sood, G. Lopez-Berestein

Analysis and interpretation of data (e.g., statistical analysis, biostatistics, computational analysis): P. Kanlikilicer, R. Mitra, C. Ivan, B. Ozpolat, G.A. Calin, A.K. Sood, G. Lopez-Berestein

Writing, review, and/or revision of the manuscript: P. Kanlikilicer, R. Mitra, A.M. Silva, B. Ozpolat, G.A. Calin, A.K. Sood, G. Lopez-Berestein
Administrative, technical, or material support (i.e., reporting or organizing data, constructing databases): R. Bayraktar, B. Aslan, C. Rodriguez-Aguayo, E. Bayraktar, B. Ozpolat, A.K. Sood, G. Lopez-Berestein
Study supervision: A.K. Sood, G. Lopez-Berestein
Other (isolation of exosomes; isolation of cellular and exosomal RNA for microarray experiment; some *in vitro* experiments like migration assay; participation in *in vivo* model work like injection, tumor collection, and preparation of tumor samples for immunohistochemical staining): M.H. Rashed

Acknowledgments

We thank Dr. Kenneth Dunner of the High-Resolution Electron Microscopy Facility.

Grant Support

This study was funded by the NIH Common Fund (UH2TR000943) through the Office of Strategic Coordination/Office of the NIH Director to G. Lopez-Berestein, A.K. Sood, G.A. Calin, and by the MD Anderson Cancer Center support grant (P30CA016672), P50 CA083639 and American Cancer Society Research Professor award to A.K. Sood, and The Center for RNA Interference and Non-Coding RNA to G.A. Calin, A.K. Sood, and G. Lopez-Berestein.

The costs of publication of this article were defrayed in part by the payment of page charges. This article must therefore be hereby marked *advertisement* in accordance with 18 U.S.C. Section 1734 solely to indicate this fact.

Received March 30, 2016; revised September 14, 2016; accepted September 23, 2016; published OnlineFirst October 14, 2016.

References

1. Johnstone RM, Adam M, Hammond JR, Orr L, Turbide C. Vesicle formation during reticulocyte maturation. Association of plasma membrane activities with released vesicles (exosomes). J Biol Chem 1987;262:9412–20.
2. Valadi H, Ekstrom K, Bossios A, Sjostrand M, Lee JJ, Lotvall JO. Exosome-mediated transfer of mRNAs and microRNAs is a novel mechanism of genetic exchange between cells. Nat Cell Biol 2007;9:654–9.
3. Braicu C, Tomuleasa C, Monroig P, Cucuianu A, Berindan-Neagoe I, Calin GA. Exosomes as divine messengers: are they the Hermes of modern molecular oncology? Cell Death Differ 2015;22:34–45.
4. Abusamra AJ, Zhong Z, Zheng X, Li M, Ichim TE, Chin JL, et al. Tumor exosomes expressing Fas ligand mediate CD8+ T-cell apoptosis. Blood Cells Mol Dis 2005;35:169–73.
5. Yang L, Wu XH, Wang D, Luo CL, Chen LX. Bladder cancer cell-derived exosomes inhibit tumor cell apoptosis and induce cell proliferation *in vitro*. Mol Med Rep 2013;8:1272–8.
6. Mineo M, Garfield SH, Taverna S, Flugy A, De Leo G, Alessandro R, et al. Exosomes released by K562 chronic myeloid leukemia cells promote angiogenesis in a Src-dependent fashion. Angiogenesis 2012; 15:33–45.
7. Taverna S, Flugy A, Saieva L, Kohn EC, Santoro A, Meraviglia S, et al. Role of exosomes released by chronic myelogenous leukemia cells in angiogenesis. Int J Cancer 2012;130:2033–43.
8. Singh R, Pochampally R, Watabe K, Lu Z, Mo YY. Exosome-mediated transfer of miR-10b promotes cell invasion in breast cancer. Mol Cancer 2014;13:256.
9. Wolfers J, Lozier A, Raposo G, Regnault A, Thery C, Masurier C, et al. Tumor-derived exosomes are a source of shared tumor rejection antigens for CTL cross-priming. Nat Med 2001;7:297–303.
10. Lee EY, Park KS, Yoon YJ, Lee J, Moon HG, Jang SC, et al. Therapeutic effects of autologous tumor-derived nanovesicles on melanoma growth and metastasis. PLoS One 2012;7:e33330.
11. Dai S, Zhou X, Wang B, Wang Q, Fu Y, Chen T, et al. Enhanced induction of dendritic cell maturation and HLA-A*0201-restricted CEA-specific CD8(+) CTL response by exosomes derived from IL-18 gene-modified CEA-positive tumor cells. J Mol Med (Berl) 2006;84:1067–76.
12. Ristorcelli E, Beraud E, Mathieu S, Lombardo D, Verine A. Essential role of Notch signaling in apoptosis of human pancreatic tumoral cells mediated by exosomal nanoparticles. Int J Cancer 2009;125:1016–26.
13. Yang Y, Xiu F, Cai Z, Wang J, Wang Q, Fu Y, et al. Increased induction of antitumor response by exosomes derived from interleukin-2 gene-modified tumor cells. J Cancer Res Clin Oncol 2007;133:389–99.
14. Falcone G, Felsani A, D'Agnano I. Signaling by exosomal microRNAs in cancer. J Exp Clin Cancer Res 2015;34:32.
15. Ohshima K, Inoue K, Fujiwara A, Hatakeyama K, Kanto K, Watanabe Y, et al. Let-7 microRNA family is selectively secreted into the extracellular environment via exosomes in a metastatic gastric cancer cell line. PLoS One 2010;5:e13247.
16. Ostenfeld MS, Jeppesen DK, Laurberg JR, Boysen AT, Bramsen JB, Primdal-Bengtson B, et al. Cellular disposal of miR23b by RAB27-dependent exosome release is linked to acquisition of metastatic properties. Cancer Res 2014;74:5758–71.
17. Bullock MD, Silva AM, Kanlikilicer-Unaldi P, Filant J, Rashed MH, Sood AK, et al. Exosomal non-coding RNAs: diagnostic, prognostic and therapeutic applications in cancer. Non-coding RNA 2015;1:53–68.
18. Lawrie CH, Gal S, Dunlop HM, Pushkaran B, Liggins AP, Pulford K, et al. Detection of elevated levels of tumour-associated microRNAs in serum of patients with diffuse large B-cell lymphoma. Br J Haematol 2008; 141:672–75.
19. Zhu W, Qin W, Atasoy U, Sauter ER. Circulating microRNAs in breast cancer and healthy subjects. BMC Res Notes 2009;2:89–89.
20. Wang J, Chen J, Chang P, LeBlanc A, Li D, Abbruzzesse JL, et al. MicroRNAs in plasma of pancreatic ductal adenocarcinoma patients as novel blood-based biomarkers of disease. Cancer Prev Res 2009;2:807–13.
21. Wittmann J, Jaeck H-M. Serum microRNAs as powerful cancer biomarkers. Biochim Biophys Acta 2010;1806:200–7.
22. Corcoran C, Friel AM, Duffy MJ, Crown J, O'Driscoll L. Intracellular and extracellular microRNAs in breast cancer. Clin Chem 2011;57:18–32.
23. Li J, Sherman-Baust CA, Tsai-Turton M, Bristow RE, Roden RB, Morin PJ. Claudin-containing exosomes in the peripheral circulation of women with ovarian cancer. BMC Cancer 2009;9:244.
24. Bala S, Petrasek J, Mundkur S, Catalano D, Levin I, Ward J, et al. Circulating microRNAs in exosomes indicate hepatocyte injury and inflammation in alcoholic, drug-induced, and inflammatory liver diseases. Hepatology 2012;56:1946–57.
25. Moreno-Smith M, Halder JB, Meltzer PS, Gonda TA, Mangala LS, Rupaimoole R, et al. ATP11B mediates platinum resistance in ovarian cancer. J Clin Invest 2013;123:2119–30.
26. Bentink S, Haibe-Kains B, Risch T, Fan JB, Hirsch MS, Holton K, et al. Angiogenic mRNA and microRNA gene expression signature predicts a novel subtype of serous ovarian cancer. PLoS One 2012;7:e30269.
27. Skog J, Wuerdinger T, van Rijn S, Meijer DH, Gainche L, Sena-Esteves M, et al. Glioblastoma microvesicles transport RNA and proteins that promote tumour growth and provide diagnostic biomarkers. Nat Cell Biol 2008;10: 1470–6.
28. Xiao D, Ohlendorf J, Chen Y, Taylor DD, Rai SN, Waigel S, et al. Identifying mRNA, microRNA and protein profiles of melanoma exosomes. PLoS One 2012;7:e46874.
29. Hoshino A, Costa-Silva B, Shen TL, Rodrigues G, Hashimoto A, Tesic Mark M, et al. Tumour exosome integrins determine organotropic metastasis. Nature 2015;527:329–35.
30. Villarroya-Beltri C, Gutierrez-Vazquez C, Sanchez-Cabo F, Perez-Hernandez D, Vazquez J, Martin-Cofreces N, et al. SUMOylated hnRNPA2B1 controls the sorting of miRNAs into exosomes through binding to specific motifs. Nat Commun 2013;4:2980.
31. Spizzo R, Nicoloso MS, Lupini L, Lu Y, Fogarty J, Rossi S, et al. miR-145 participates with TP53 in a death-promoting regulatory loop and targets estrogen receptor-alpha in human breast cancer cells. Cell Death Differ 2010;17:246–54.
32. Tessel MA, Krett NL, Rosen ST. Steroid receptor and microRNA regulation in cancer. Curr Opin Oncol 2010;22:592–97.
33. Grange C, Tapparo M, Collino F, Vitillo L, Damasco C, Deregibus MC, et al. Microvesicles released from human renal cancer stem cells stimulate

angiogenesis and formation of lung premetastatic niche. Cancer Res 2011;71:5346–56.
34. Roccaro AM, Sacco A, Maiso P, Azab AK, Tai YT, Reagan M, et al. BM mesenchymal stromal cell-derived exosomes facilitate multiple myeloma progression. J Clin Invest 2013;123:1542–55.
35. Cho JA, Park H, Lim EH, Lee KW. Exosomes from breast cancer cells can convert adipose tissue-derived mesenchymal stem cells into myofibroblast-like cells. Int J Oncol 2012;40:130–8.
36. Tanaka Y, Kamohara H, Kinoshita K, Kurashige J, Ishimoto T, Iwatsuki M, et al. Clinical impact of serum exosomal microRNA-21 as a clinical biomarker in human esophageal squamous cell carcinoma. Cancer 2013;119:1159–67.
37. Berry MG, Goode AW, Puddefoot JR, Vinson GP, Carpenter R. Integrin beta1-mediated invasion of human breast cancer cells: an *ex vivo* assay for invasiveness. Breast Cancer 2003;10:214–9.
38. Arao S, Masumoto A, Otsuki M. Beta1 integrins play an essential role in adhesion and invasion of pancreatic carcinoma cells. Pancreas 2000; 20:129–37.
39. Masumoto A, Arao S, Otsuki M. Role of beta1 integrins in adhesion and invasion of hepatocellular carcinoma cells. Hepatology 1999;29:68–74.
40. Schwartz MA, Assoian RK. Integrins and cell proliferation: regulation of cyclin-dependent kinases via cytoplasmic signaling pathways. J Cell Sci 2001;114:2553–60.
41. Zhang X, Shi H, Tang H, Fang Z, Wang J, Cui S. miR-218 inhibits the invasion and migration of colon cancer cells by targeting the PI3K/Akt/mTOR signaling pathway. Int J Mol Med 2015;35:1301–8.
42. Dillon RL, White DE, Muller WJ. The phosphatidyl inositol 3-kinase signaling network: implications for human breast cancer. Oncogene 2007; 26:1338–45.
43. Ye M, Hu DN, Tu LL, Zhou XT, Lu F, Wen B, et al. Involvement of PI3K/Akt signaling pathway in hepatocyte growth factor - induced migration of uveal melanoma cells. Invest Ophth Vis Sci 2008;49:497–504.
44. Shulkla S, MacLennan GT, Hartman DJ, Fu P, Resnick MI, Gupta S. Activation of PI3K-Akt signaling pathway promotes prostate cancer cell invasion. Int J Cancer 2007;121:1424–32.
45. Karar J, Maity A. PI3K/AKT/mTOR pathway in angiogenesis. Front Mol Neurosci 2011;4:51.
46. Garcia-Echeverria C, Sellers WR. Drug discovery approaches targeting the PI3K/Akt pathway in cancer. Oncogene 2008;27:5511–26.
47. Fujita Y, Yagishita S, Hagiwara K, Yoshioka Y, Kosaka N, Takeshita F, et al. The clinical relevance of the miR-197/CKS1B/STAT3-mediated PD-L1 network in chemoresistant non-small-cell lung cancer. Mol Ther 2015;23: 717–27.
48. Milane L, Singh A, Mattheolabakis G, Suresh M, Amiji MM. Exosome mediated communication within the tumor microenvironment. J Control Release 2015;219:278–94.
49. Riches A, Campbell E, Borger E, Powis S. Regulation of exosome release from mammary epithelial and breast cancer cells - A new regulatory pathway. Eur J Cancer 2014;50:1025–34.
50. Gercel-Taylor C, Atay S, Tullis RH, Kesimer M, Taylor DD. Nanoparticle analysis of circulating cell-derived vesicles in ovarian cancer patients. Anal Biochem 2012;428:44–53.